

Ultrasound and magnetic resonance imaging of cyclic arginine glycine aspartic acid-gadopentetic acid-poly(lactic acid) in human breast cancer by targeting $\alpha\text{v}\beta 3$ in xenograft-bearing nude mice

Danhui Fu^{a,b,c,*}, Xiangyang Huang^{a,b,c,*}, Zheng Lv^{d,*}, Yupeng Zhang^d, Miao Chen^{a,b,c}, Wei Zhang^e, and Danke Su^{a,b,c}

^aDepartments of Radiology, Guangxi Medical University Cancer Hospital, Nanning, Guangxi, China; ^bMedical Imaging Department, Guangxi Key Clinical Specialty, China; ^cMedical Imaging Department, Dominant Cultivation Discipline of Guangxi Medical University Cancer Hospital; ^dGraduate School, Guilin Medical University, Guilin, Guangxi, China; ^eDepartment of Radiology, Liuzhou People's Hospital Affiliated to Guangxi Medical University, Liuzhou, Guangxi, China

ABSTRACT

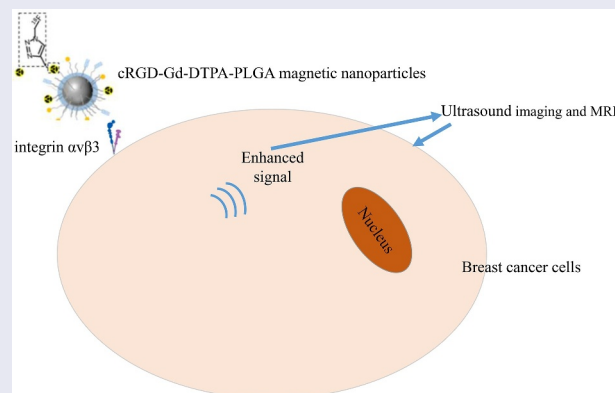
Effective early detection shows the potential to reduce breast cancer mortality. This study aimed to establish a targeted contrast agent for Magnetic Resonance Imaging (MRI)/ultrasound dual-modality molecular radiography for breast cancer. The cyclic arginine-glycine-aspartate-gadopentetic acid-poly(lactic acid) (cRGD and Gd-DTPA) coated by multi-functional blank poly(lactic-co-glycolic acid) (PLGA) nanoparticles) was successfully constructed by chemical synthesis method with high stability. The safety of cRGD-Gd-DTPA-PLGA was demonstrated in vitro and in vivo, and their affinity to breast cancer cells was revealed. Moreover, MRI/ultrasound dual-modality molecular radiography in vitro showed that as the concentration of contrast agent increased, the echo enhancement and signal intensity of MRI imaging were also elevated. The mouse models of human breast cancer also indicated significant target enhancements of cRGD-Gd-DTPA-PLGA magnetic nanoparticles in the mouse tumor. Thus, cRGD-Gd-DTPA-PLGA magnetic nanoparticles were suggested as qualified MRI/ultrasound dual-modality molecular radiography contrast agent. We further explored the targeting mechanism of cRGD-Gd-DTPA-PLGA in breast cancer. The results showed that $\alpha\text{v}\beta 3$ was highly expressed in breast cancer tissues, and cRGD-Gd-DTPA-PLGA used for MRI/ultrasound dual-modality molecular radiography by targeting $\alpha\text{v}\beta 3$. Additionally, we found that the signal-to-noise ratio of MRI was positively correlated with microvessel density (MVD). The cRGD-Gd-DTPA-PLGA dynamically and quantitatively monitored breast cancer by monitoring the state of neovascularization. In conclusion, in the present study, we successfully constructed the cRGD-Gd-DTPA-PLGA magnetic nanoparticles for MRI/ultrasound dual-modality molecular radiography. The cRGD-Gd-DTPA-PLGA showed potential in early detection and diagnosis of metastasis, and dynamic evaluation of the efficacy of molecular targeted therapy of integrin $\alpha\text{v}\beta 3$.

ARTICLE HISTORY

Received 8 December 2021
Revised 17 February 2022
Accepted 18 February 2022

KEYWORDS

Breast cancer; ultrasound; magnetic resonance imaging; cRGD-Gd-DTPA-PLGA; $\alpha\text{v}\beta 3$



CONTACT Danke Su  sudanke33@sina.com, holly2yang@126.com; Wei Zhang  Departments of Radiology, Guangxi Medical University Cancer Hospital, No. 71 Hedi Road, Nanning, China.

*These authors contributed equally to this work.

© 2022 The Author(s). Published by Informa UK Limited, trading as Taylor & Francis Group.
This is an Open Access article distributed under the terms of the Creative Commons Attribution-NonCommercial License (<http://creativecommons.org/licenses/by-nc/4.0/>), which permits unrestricted non-commercial use, distribution, and reproduction in any medium, provided the original work is properly cited.

Introduction

Breast cancer is the most common female malignant tumor and the leading cause of cancer death in women [1]. The incidence of breast cancer are rising, especially in some economically developed regions, and tends to occur in younger women [2]. With the deepening of breast cancer tumor marker research, the development of imaging diagnostic technology and the continuous advancement of omics technology, the diagnostic level of breast cancer has improved [3,4]. However, effective methods for the early specific diagnosis of breast cancer remain to be investigated. The early detection and standardize diagnosis to reduce mortality of breast cancer is still a major challenge.

Imaging is a choice in lung and breast cancer population screening programs. In clinical imaging examinations of breast cancer, ultrasound is real-time, fast, convenient, and safe imaging method for examination and monitoring, commonly used in routine clinical diagnosis. Ultrasound imaging can visualize small cancers clinically and mammographically hidden in dense breasts [5,6]. Magnetic resonance imaging (MRI) with good soft tissue resolution can evaluate breast tissue density and morphological changes. MRI is a highly sensitive for all breast cancers, and has a modality-based advantage compared with sonography and mammography in early examination of invasive breast cancer [7,8]. However, the inspection lasts longer and cannot be imaged in real time, and the patients accessible to MRI are limited [8]. Therefore, by integrating the application of ultrasound and MRI, we expect to improve the efficacy of breast cancer diagnosis as well as preserve the diagnostic accuracy.

The development of multimodel imaging and molecular biology have provided new opportunities for the exploration of new imaging agents of biomedical imaging. Ultrasound contrast agents are biocolloids acting as echo-enhancers under an ultrasound field. There are various types of ultrasound contrast agents, including microbubbles, nanobubbles, nanodrops, and echogenic liposomes. Microbubbles and nanobubbles are mainly comprised of phospholipids, gas, sulfur hexafluoride, and fluorocarbon [9]. In spite of the wide application of the microsized contrast agents,

their short in vivo half-life results in insufficient imaging frames of the target, while nanoparticles show longer tumor enhancement time compared to microbubbles in vivo [10]. New polymer materials, such as poly(lactic-co-glycolic acid) (PLGA), has also been used to prepare the shell of the contrast agent with good compression resistance and high stability [11,12]. Thus, in this study, we constructed the contrast agent cRGD-Gd-DTPA-PLGA magnetic nanoparticles for the first time and investigated its practicability for magnetic resonance/ultrasound bimodal molecular imaging of breast cancer. We used both in vitro and in vivo assays and revealed the targeting mechanism of cRGD-Gd-DTPA-PLGA magnetic nanoparticles used for MRI/ultrasound imaging. The exploration and advancement of contrast agents may promote the development of MRI/ultrasound imaging and the early diagnosis of breast cancer.

Integrin $\alpha\beta3$ receptors are highly expressed on the surface of various malignant tumor cells, especially in the neovascular endothelial cell membrane of malignant tumor tissues, while in mature vascular endothelial cells and most normal organ systems $\alpha\beta3$ are not expressed and can hardly be detected [13]. Small molecule peptides containing arginine-glycine-aspartic acid (RGD) sequence are integrin $\alpha\beta3$ receptor antagonists, with a high degree of selectivity and affinity for integrin $\alpha\beta3$ receptors, are a class of tumor receptor imaging agent with potential clinical application value [14,15].

This study aimed to investigate the suitability and practicability of cRGD-Gd-DTPA-PLGA nanoparticles as the targeted contrast agent for MRI/ultrasound dual-modality molecular radiography in breast cancer. We assumed that cRGD-Gd-DTPA-PLGA magnetic nanoparticles used for MRI/ultrasound imaging by targeting $\alpha\beta3$. This study may provide prospects in the early diagnosis of breast cancer.

Materials and methods

Construction of cRGD-Gd-DTPA-PLGA

The cRGD-Gd-DTPA-PLGA was constructed based on the previous studies [16]. The sodium

periodate (NaIO₄, 11.1 mg) was distilled in 0.2 ml of distilled water and mixed thoroughly. Then, 1 ml of Gd-DTPA was added to NaIO₄ solution and shake well at room temperature for 30 min. Next, the mix was immediately reduced by 1 ml of ethylene glycol reducing solution and placed at room temperature for 30 min, then 5 mg cRGD was added, mixed overnight, and added into 100 µl of sodium borohydride solution, placed it in a refrigerator at 4°C for 2 h to obtain the targeted molecular probe cRGD-Gd-DTPA. Finally, the cRGD-Gd-DTPA was lotus with polylactic acid to finish the construction of cRGD-Gd-DTPA-PLGA. Transmission electron microscopy (TEM) was used to detect the phenotype of cRGD-Gd-DTPA-PLGA. Nanocapsule particle size was determined by Nicomp 380 ZLS particle size-potentiometer at 25°C with light intensity to 300 ± 20 KHz.

Transmission electron microscopy

The cRGD-Gd-DTPA-PLGA was washed briefly with PBS and fixed in 2.5% glutaraldehyde in 0.1 M phosphate buffer (pH 7.4) at room temperature for 30 min. Next, the pellets were post-fixed in 2.0% osmium tetroxide in 0.1 M phosphate buffer at 4°C for 2 h, dehydrated in ethanol followed by acetone and embedded in LX-112 (Ladd, USA). Samples were contrasted with uranyl acetate followed by lead citrate and examined in a Hitachi HT7700 (Tokyo, Japan) at 80 kV. Digital images were taken using a Veleta camera (Olympus, Germany).

In vitro ultrasound and magnetic resonance imaging (MRI)

The MRI dual-modality imaging in vitro was performed as previously reported [17]. A series of samples were prepared using PBS buffer solution in various concentrations, including 0, 5, 10, 20, 40, and 80 µM. After being fully dispersed by ultrasonic in a water bath, the samples have been combined with the control sample PBS buffer. Ultrasound imaging was performed by Aplio500 color Doppler ultrasound system. MRI was performed by GE Discovery 750 under 3 T magnetic field strength. A small animal coil was used to

scan with the following parameters: field of view area 25 mm × 62 mm, layer thickness 1.0 mm, repetition time (TR) = 5000 ms, back wave time (TE) = 10.6 ms-53 ms. The sequence multicontrast-spin echo was pulsed, and the scan data was recorded and reconstructed to obtain the T₂-weighted MRI image. Finally, the results were recorded and the corresponding transverse relaxation time (T₂ value) and the relaxation rate (r₂) of the sample were calculated.

Cell line, culture and treatment

Human breast cancer cell line MCF-7 and MDA-MB-435S cells and the normal breast cell MCF10A line were purchased from the American Type Culture Collection (ATCC). Cells were cultured in DMEM medium supplemented with 10% fetal bovine serum (FBS, Gibco, USA) under 37°C with 5% CO₂. For further experiment, MCF-7 and MDA-MB-435S cells were incubated for 1 h at 37°C in an incubator containing 5% CO₂ under 95% saturation humidity under treatment of cRGD-Gd-DTPA-PLGA.

Cytotoxicity analysis of cRGD-Gd-DTPA-PLGA

Cytotoxicity of cRGD-Gd-DTPA-PLGA to cells was examined by a MTT assay in vitro [18]. Briefly, 1 × 10⁶ MCF-7 cells were incubated in a 96-well plate and the cells were harvested at 0, 12 h, 24 h, and 48 h after incubation with cRGD-Gd-DTPA-PLGA. Then, 100 µL of cell suspension were incubated with 10 µL of MTT for 4 h after washing with PBS. The absorbance was detected in the 96-well plate by a microplate reader at 450 nm. For in vivo assays, 20 healthy mice were randomly divided into 2 groups, including control and cRGD-Gd-DTPA-PLGA group in different concentrations, respectively. Blood routine examination and liver and kidney function analysis were performed. Histopathological analyses of liver, kidney, and other important organs were detected by H&E staining.

Analysis of avβ3 affinity

The MCF-7 cells (1 × 10⁶ cells) were cultured in DMEM medium supplemented with 10% fetal

bovine serum (FBS, Gibco, USA) under 37°C with 5% CO₂. The cells were treated with DiI-labeled cRGD-Gd-DTPA-PLGA when they reached 70–90% confluence and continued the incubation for 12 h. Then the fluorescence was detected by a fluorescence microscope (Olympus). Flow cytometry analysis was used to detect the affinity between cRGD-Gd-DTPA-PLGA magnetic nanoparticles and MCF-7 cells and MDA-MB-435S cells.

Tumor-bearing nude mouse model of human breast cancer

Fifteen female weighted 20–25 g at 10 weeks were purchased from Beijing Vital River Laboratory Animal Technology Co., Ltd., (Beijing, China) and bred in SPF animal laboratory at 21–23°C under a 12 h light and dark cycle. Tumor-bearing nude mouse model was established by injecting subcutaneously with 100 µL MCF-7 cells (5×10^7 cells/mL) in the anterior shoulder [19]. Subsequently, the tumor-bearing nude mice were injected with cRGD-Gd-DTPA-PLGA magnetic nanoparticles at 14 days after model establishment by tail vein injection. Then the nude mice were selected for ultrasound and MRI. All the experiments were approved by the Ethics Committee our school (GLMC202003011).

In vivo ultrasound and magnetic resonance imaging

The animals were anesthetized by intraperitoneal injection of 3% sodium pentobarbital (1 ml/100 g). The ultrasound treatment of the tumor was assessed using GE Vivid E7 ultrasonic diagnostic equipment, ML6-15 probe, frequency 15 MHz, imaging depth 2 cm. MRI was performed on a 3.0 T MRI scanner (GE Discovery MR 750, 3.0 T). In order to obtain the maximum signal-to-noise ratio image, the orthogonal knee joint coil was adopted. The scan sequence used time-of-flight (TOF) 3D fast gradient echo sequence. Parameters were as follows: TR/TE = 22/5.7 ms, excitation angle = 15°, FOV = 8 cm × 6 cm, matrix = 512 × 512, layer thickness = 1.2 mm. Contrast to noise ratio (CNR) was used to measure and analyze the video intensity before and after

contrast. $CNR = ROI \text{ signal intensity} - \text{signal intensity of surrounding muscle tissue} / \text{background noise signal intensity}$.

Hematoxylin-eosin (H&E) staining

The mouse tissues from different organs after different treatment were obtained and sliced into 4 µm sections and embedded in paraffin. For H&E staining [20], deparaffinized sections were stained with hematoxylin staining solution for 3–5 min followed by differentiation, return blue, and then the slices were rinsed with running water. Next, they were stained with eosin staining solution for 5 min after being dehydrated with 85% and 95% gradient alcohol for 5 min. Finally, the slices were dehydrated and sealed with neutral gum. Images in different fields were taken by a microscope (Olympus).

Immunofluorescence staining

Immunofluorescence staining was used to detect the expression and distribution of $\alpha v \beta 3$ and CD31 in breast cancer tumor tissues as previously described [21]. Briefly, frozen section of tumor tissue was fixed with 4% paraformaldehyde, embedded in paraffin and sliced into 4 µm sections. After being blocked with 10% goat serum for 15 min, the sections were then incubated with primary antibodies including anti- $\alpha v \beta 3$ (Abcam) and anti-CD31 (Abcam) overnight at 4°C. Subsequently, the cells were incubated with the secondary antibody Goat Anti-Mouse IgG H&L (Alexa Fluor® 488) (Abcam) for 1 h at 37°C in the dark. Then, the slices were counterstained with 0.1 µg/ml Hoechst (Sigma-Aldrich) for 5 min. Images were taken using a fluorescent microscope (OLYMPUS, IX71). Microvessel density (MVD) was calculated by the CD31 immunofluorescence signal.

Statistical analysis

The data were presented as the mean ± standard deviation (SD) and analyzed by SPSS 19.0 software (SPSS Inc., USA). Differences between two groups and among more than two groups were analyzed using unpaired *t* test and one-way analysis of variance (ANOVA), respectively. $P < 0.05$ was considered statistically significant.

Results

In this study, we constructed the cRGD-Gd-DTPA-PLGA nanoparticles and investigated their role as the targeted contrast agent for MRI/ultrasound dual-modality molecular radiography. We hypothesized that cRGD-Gd-DTPA-PLGA magnetic nanoparticles were used in MRI/ultrasound imaging by targeting $\alpha v\beta 3$. The results of in vitro and in vivo assays indicated that cRGD-Gd-DTPA-PLGA nanoparticles were safe and stable contrast agents, which bound to the breast cancer cells in vitro, and showed qualified results in MRI/ultrasound dual-modality molecular radiography. Moreover, in the breast cancer mouse model, cRGD-Gd-DTPA-PLGA was demonstrated to target $\alpha v\beta 3$. The positive correlation between signal-to-noise ratio of MRI and microvessel density (MVD) also suggested the role of cRGD-Gd-DTPA-PLGA to monitor breast cancer progression via reflecting the state of neovascularization.

Characteristic analysis of cRGD-Gd-DTPA-PLGA magnetic nanoparticles

The cRGD-Gd-DTPA-PLGA magnetic nanoparticles were successfully constructed according to the synthetic pathway shown in Figure 1). Transmission electron microscope (TEM) analysis indicated that

the cRGD-Gd-DTPA-PLGA magnetic nanoparticles were spherical and numbers of Gd particles were evenly distributed in the shell structure (Figure 1)) with an average size about 31 ± 2.87 nm detected by Nicomp 380 ZLS particle size-potentiometer (Figure 1)). The longitudinal (r_1) and transversal (r_2) relaxivities of cRGD-Gd-DTPA-PLGA magnetic nanoparticles were shown in Figure 1).

Safety assessment of cRGD-Gd-DTPA-PLGA magnetic nanoparticles

In order to ensure the safety of cRGD-Gd-DTPA-PLGA magnetic nanoparticles, cytotoxicity of cRGD-Gd-DTPA-PLGA magnetic nanoparticles was measured both in vitro and in vivo. The results of MTT assay showed that the proliferation of MCF-7 cells was not significantly affected after the treatment of different concentrations of cRGD-Gd-DTPA-PLGA magnetic nanoparticles, including 0, 10, 20, 40, and 80 μM (Figure 2)). Flow cytometry analysis indicated that the apoptosis rate of breast cancer cells was less than 10% when the concentration of cRGD-Gd-DTPA-PLGA magnetic nanoparticles reached 80 μM (Figure 2)). H&E staining analysis indicated that all tissues and organs presented normal cell morphology, clear boundary,

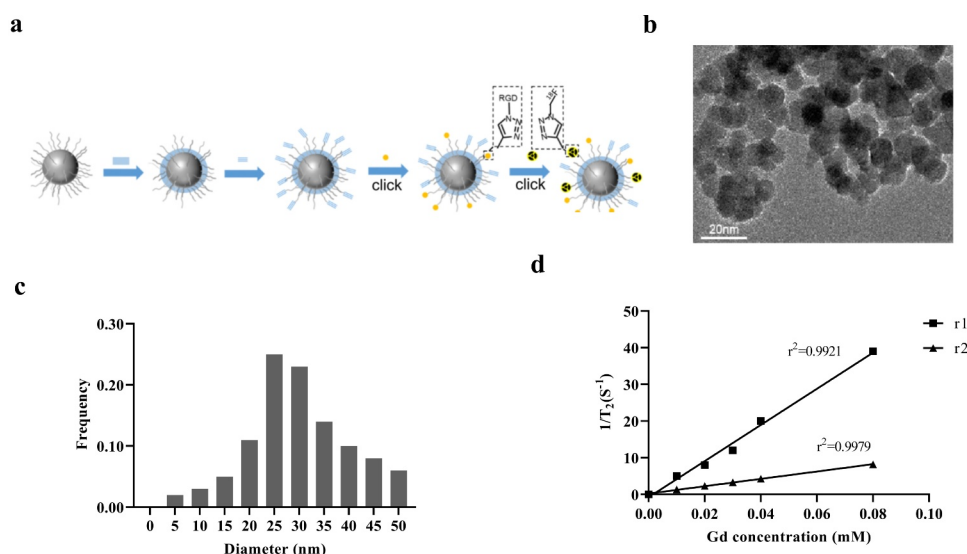


Figure 1. Characteristic analysis of cRGD-Gd-DTPA-PLGA magnetic nanoparticles.

A, Synthetic pathway of cRGD-Gd-DTPA-PLGA magnetic nanoparticles; B, TEM analysis was used to detect the phenotype of cRGD-Gd-DTPA-PLGA magnetic nanoparticles; C, Average size of cRGD-Gd-DTPA-PLGA magnetic nanoparticles was detected by Nicomp 380 ZLS particle size-potentiometer; D, The longitudinal (r_1) and transversal (r_2) relaxivities of cRGD-Gd-DTPA-PLGA magnetic nanoparticles.

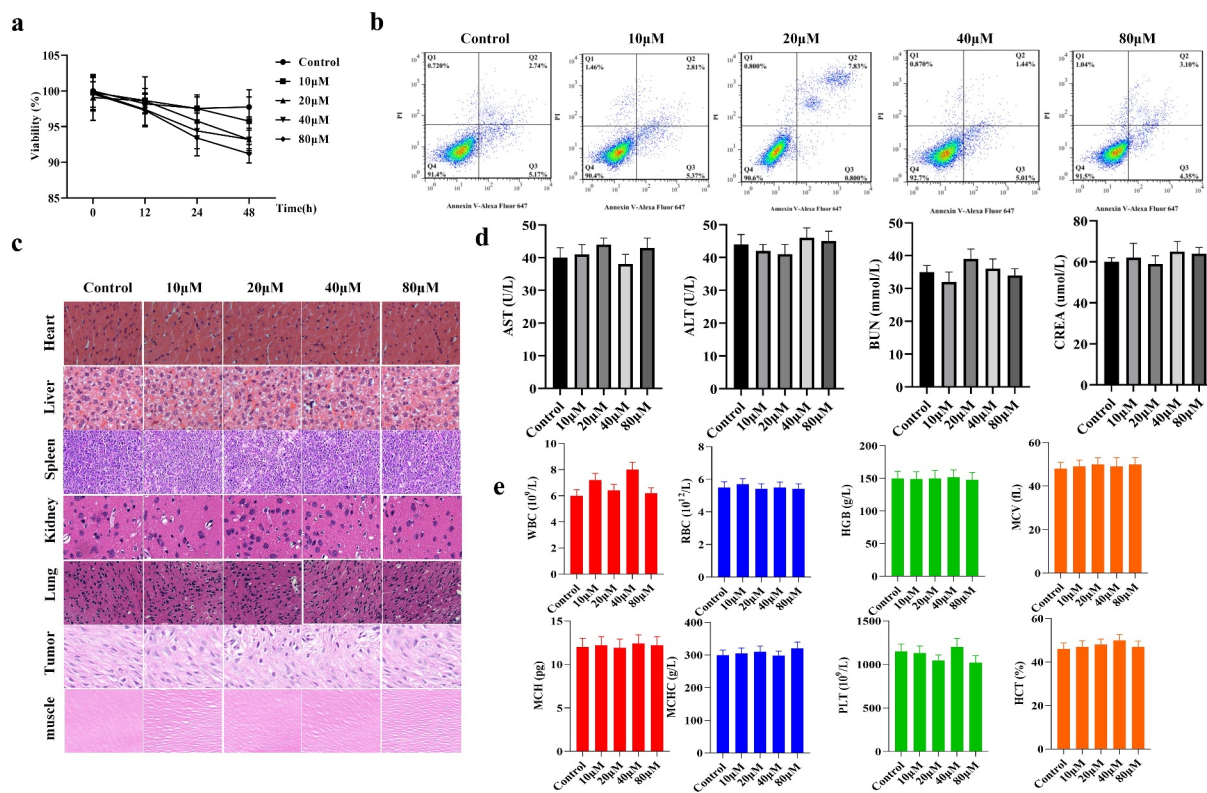


Figure 2. Safety assessment of cRGD-Gd-DTPA-PLGA magnetic nanoparticles.

A, MTT was used to detect the proliferation of MCF-7 cells treated with different concentration of cRGD-Gd-DTPA-PLGA magnetic nanoparticles, including 0, 10, 20, 40, and 80 μM ; B, Flow cytometry analysis was used to detect the apoptosis with different concentrations of cRGD-Gd-DTPA-PLGA magnetic nanoparticles; C, H&E staining was used to detect the inflammation and cell injury of heart, liver, spleen, kidney, lung, tumor and muscle; D, The contents of ALT, AST, BUN, and CREA in serum after the treatment with different concentrations of cRGD-Gd-DTPA-PLGA magnetic nanoparticles; E, The blood routine, liver and kidney function affected in all mice treated with different concentrations of cRGD-Gd-DTPA-PLGA magnetic nanoparticles.

and orderly tissue structure without inflammation and cell injury, including heart, liver, spleen, kidney, lung, tumor, and muscle (Figure 2)). Furthermore, we found that the contents of alanine aminotransferase (ALT), aspartate aminotransferase (AST), urea nitrogen (BUN), and creatinine (CREA) in serum were not significantly changed under the treatment of different concentrations of cRGD-Gd-DTPA-PLGA magnetic nanoparticles compared with the control group (Figure 2)). In addition, the blood routine, liver, and kidney functions were also not affected in all mouse groups treated with different concentrations of cRGD-Gd-DTPA-PLGA magnetic nanoparticles (Figure 2)). These results indicated that cRGD-Gd-DTPA-PLGA magnetic nanoparticles are safe contrast agents.

Ability of cRGD-Gd-DTPA-PLGA to bind with tumor cells in vitro

The binding ability of cRGD-Gd-DTPA-PLGA to MCF-7 and MDA-MB-435S cells was observed via laser confocal microscopy, with MCF10A cells as the control group. As shown in Figure 3), a large number of DiI-labeled cRGD-Gd-DTPA-PLGA nanoparticles were observed around MCF-7 and MDA-MB-435S cell membranes. In contrast, no DiI labeled cRGD-Gd-DTPA-PLGA nanoparticles were found around MCF10A cells. Flow cytometry analysis showed that the affinity of cRGD-Gd-DTPA-PLGA magnetic nanoparticles to MCF-7 and MDA-MB-435S cells was significantly higher than to MCF10A cells (Figure 3)).

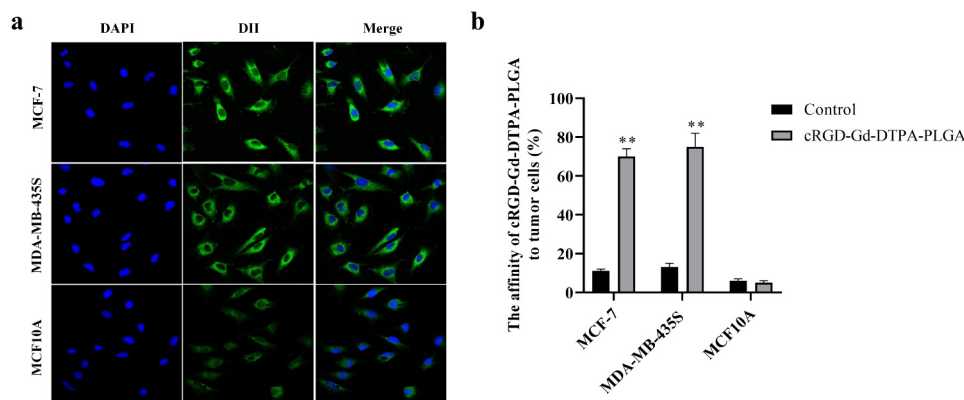


Figure 3. Ability of cRGD-Gd-DTPA-PLGA to bind tumor cells in vitro.

A, Laser confocal microscope was used to observe cRGD-Gd-DTPA-PLGA magnetic nanoparticles binding to MCF-7 and MDA-MB-435S cells; B, Flow cytometry analysis was used to detect the affinity of cRGD-Gd-DTPA-PLGA magnetic nanoparticles to MCF-7 and MDA-MB-435S cells. ** $P < 0.01$ vs. Control.

In vitro MRI/ultrasound dual-modality molecular radiography

To explore the ability of cRGD-Gd-DTPA-PLGA magnetic nanoparticles as MRI/ultrasound contrast agent, the MRI/ultrasound dual-modality molecular radiography in vitro was performed. The results of ultrasound imaging showed obvious echo enhancement in the lumen, which was manifested as dense, fine dot-like strong echoes, and no obvious sound shadow was observed in the rear. The echo enhancement in the form of fine dots continued to increase as the concentration of the contrast agent increased (Figure 4). The MRI imaging with cRGD-Gd-DTPA-PLGA magnetic nanoparticles under 3 T magnetic field strength showed a higher signal intensity in the T2-weighted image and the T1/T2 value increased as the concentration of the contrast agent

increased (Figure 4)). The r value of cRGD-Gd-DTPA-PLGA was 0.9778 (Figure 4)). The results of the MRI in vitro indicated that cRGD-Gd-DTPA-PLGA magnetic nanoparticles are qualified MRI/ultrasound dual-modality molecular radiography contrast agent.

In vivo MRI/ultrasound dual-modality molecular radiography

We further investigated the function of cRGD-Gd-DTPA-PLGA magnetic nanoparticles as MRI/ultrasound contrast agent in vivo. The cRGD-Gd-DTPA-PLGA magnetic nanoparticles were injected into tumor-bearing mice via the vena caudalis at 42 $\mu\text{mol Gd/kg}$. Mice were scanned at 15 min, 30 min, 1 h, 2 h, and 3 h following the contrast injection. The results of ultrasound imaging indicated that the contrast enhancement was

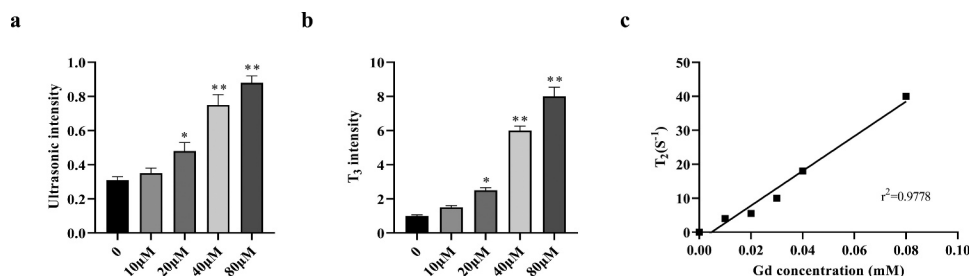


Figure 4. In vitro MRI/ultrasound dual-modality molecular radiography.

A, Ultrasound imaging detected by the Aplio 500 ultrasound imaging system with different concentrations of cRGD-Gd-DTPA-PLGA magnetic nanoparticles; B, The MRI imaging with cRGD-Gd-DTPA-PLGA magnetic nanoparticles under 3 T magnetic field strength; C, The r value of cRGD-Gd-DTPA-PLGA in the T2-MRI imaging. * $P < 0.05$, ** $P < 0.01$ vs. 0 μM .

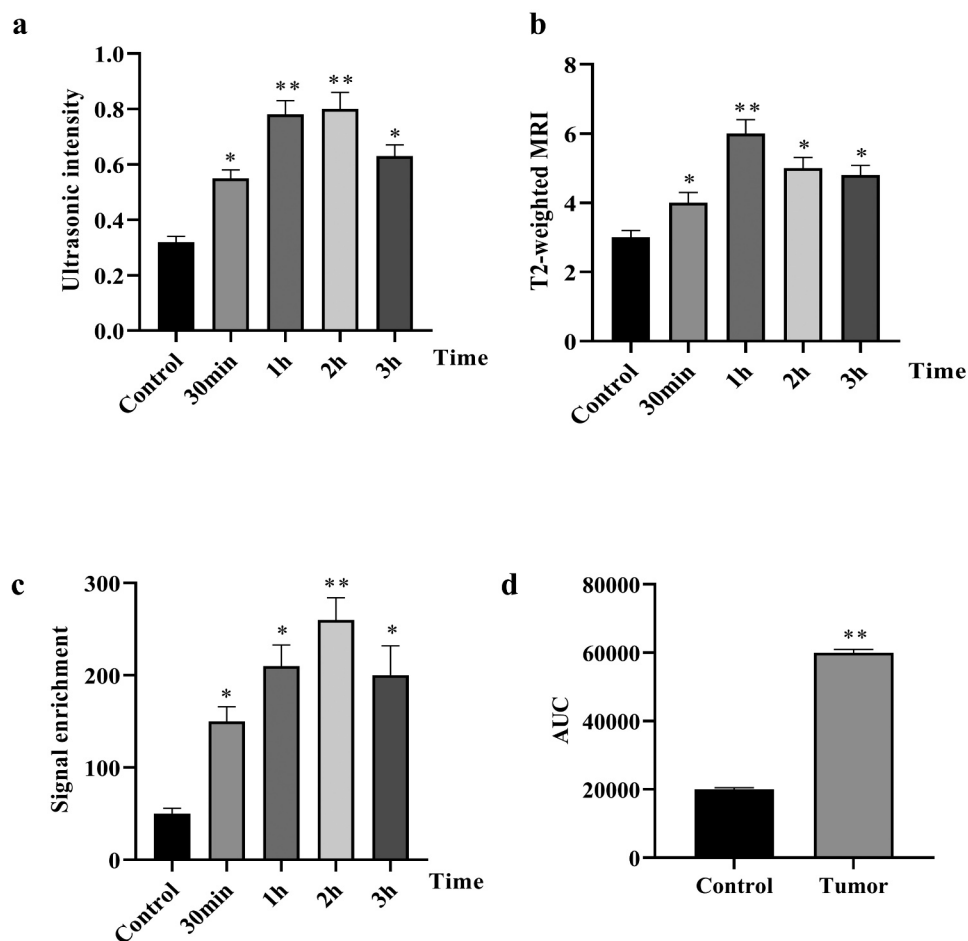


Figure 5. In vivo MRI/ultrasound dual-modality molecular radiography.

A, Ultrasound imaging with cRGD-Gd-DTPA-PLGA contrast scanned at 15, 30 min, 1, 2 and 3 h following contrast injection; B, T2-weighted MRI for the tumor at 15, 30 min, 1, 2, and 3 h following contrast injection; C, The signal-to-noise ratio of the tumor; D, The enhanced signal-time curve (AUC) of cRGD-Gd-DTPA-PLGA was calculated by the trapezoidal method. * $P < 0.05$, ** $P < 0.01$ vs. Control.

uniform and fine, and the tumor outline was clear and complete. The contrast intensity increased as time increased compared with the control group (Figure 5). T2-weighted MRI showed that the tumor signal was brighter than that of the other tissues. The tumor boundary was also distinct and the signal intensities of the tumors were enhanced to a maximum 1 h after injection, and then gradually decreased (Figure 5). The signal-to-noise ratio of the tumor was maximal 2 h after injection and then gradually decreased (Figure 5). The enhanced signal-time curve (AUC) of cRGD-Gd-DTPA-PLGA was calculated by the trapezoidal method. The results showed that cRGD-Gd-DTPA-PLGA exhibited significant target enhancements in the tumor as contrast agent for MRI/ultrasound (Figure 5).

The cRGD-Gd-DTPA-PLGA was used for MRI by targeting $\alpha v \beta 3$

The targeting mechanism of cRGD-Gd-DTPA-PLGA used for MRI/ultrasound dual-modality molecular radiography was further explored. Colocalization analysis between cRGD-Gd-DTPA-PLGA and $\alpha v \beta 3$ distribution in vivo was performed. H&E staining analysis showed the inflammatory cell infiltration in tumor tissues (Figure 6). Western blot analysis showed that the protein expression of $\alpha v \beta 3$ was significantly elevated in the breast cancer tumor tissues compared with the control group (Figure 6). Further analysis indicated that cRGD-Gd-DTPA-PLGA uptake and $\alpha v \beta 3$ expression were significantly increased in the tumor bearing mice

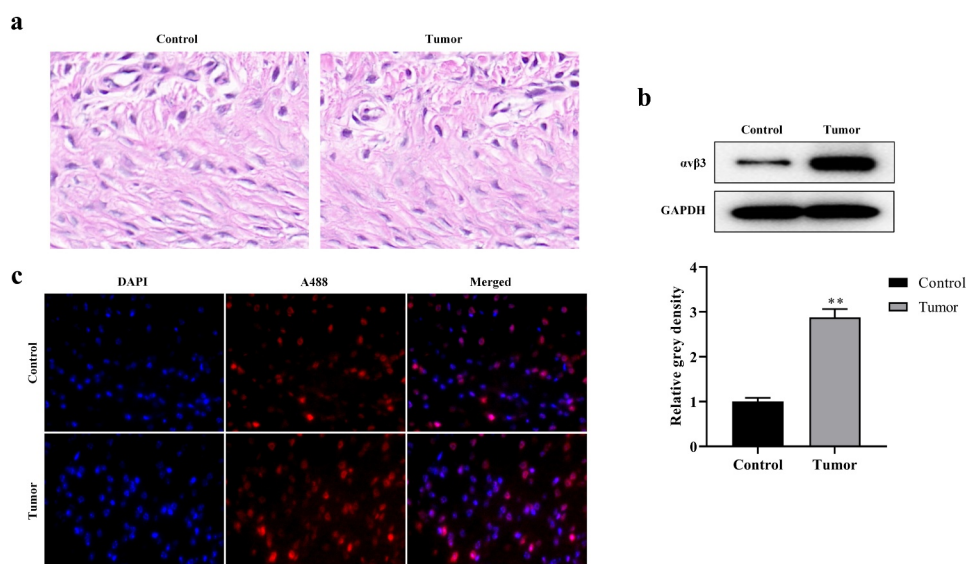


Figure 6. The cRGD-Gd-DTPA-PLGA used for MRI by targeting $\alpha\text{v}\beta 3$.

A, H&E staining was used to detect the inflammatory cell infiltration in tumor tissues; B, Western blot analysis was used to detect the protein expression of $\alpha\text{v}\beta 3$ in the tumor tissues; C, MRI signal with cRGD-Gd-DTPA-PLGA and the immunofluorescence signal of $\alpha\text{v}\beta 3$ in the tumor bearing mice. $**P < 0.01$ vs. Control.

group compared with the control group. Moreover, the signal of cRGD-Gd-DTPA-PLGA was overlapped with the immunofluorescence signal of $\alpha\text{v}\beta 3$ (Figure 6), which suggested that the cRGD-Gd-DTPA-PLGA was used for MRI/ultrasound dual-modality molecular radiography by targeting $\alpha\text{v}\beta 3$.

Correlation analysis between signal-to-noise ratio of MRI and microvessel density (MVD)

To explore the correlation between signal-to-noise ratio of MRI and MVD, the correlation analysis between signal-to-noise ratio of MRI and MVD was performed. As shown in Figure 7), the results of CD31 immunofluorescence staining analysis showed that the expression of CD31 was increased in the tumor tissues compared with the control group. According to the fluorescence signaling, MVD was also significantly elevated in breast cancer tumor compared with the control group (Figure 7)). Correlation analysis between signal-to-noise ratio of MRI and MVD showed that the signal-to-noise ratio of MRI is positively correlation with MVD (Figure 7)), which indicated that cRGD-Gd-DTPA-PLGA dynamically and quantitatively monitored breast

cancer progression in mouse models by reflecting the state of neovascularization.

Discussion

Increasing studies have revealed the advancement in the treatment of breast cancer due to the in-depth research on cancer pathogenesis [22]. However, effective methods for the early specific diagnosis of breast cancer remain to be explored. Molecular imaging technology, with the advantages of non-invasiveness and high specificity, can realize the early and specific diagnosis of diseases at the molecular and cellular level, plays an important role in the diagnosis of tumors [23]. In the present study, we established cRGD-Gd-DTPA-PLGA magnetic nanoparticles which were used for MRI/ultrasound dual-modality molecular radiography in breast cancer mouse models by targeting $\alpha\text{v}\beta 3$.

The exploration of contrast agents promotes the development of MRI/ultrasound imaging and the early diagnosis of breast cancer. Multi-labeled particles are demanded because they can combine the strengths of different diagnostic methods, such as MRI and ultrasound [24,25]. The Gadolinium (Gd) with paramagnetic properties and shortened the T_1 relaxation times of hydrogens in

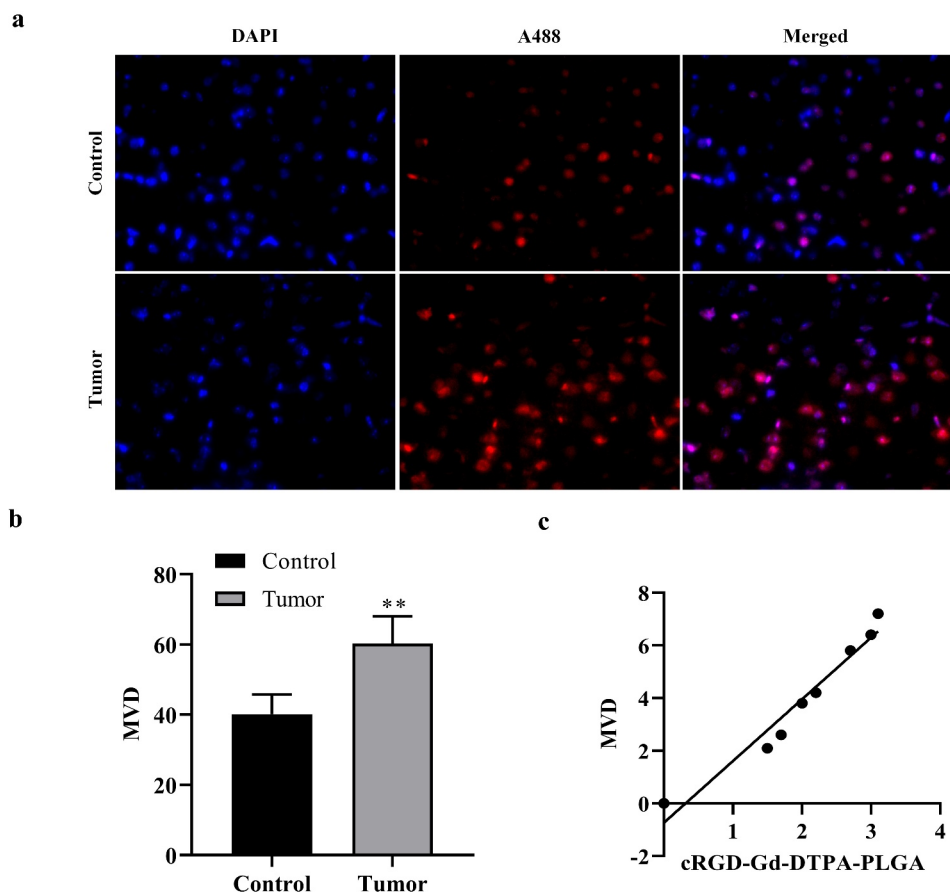


Figure 7. Correlation analysis between signal-to-noise ratio of MRI and microvessel density (MVD).

A, Immunofluorescence staining was used to detect the expression of CD31; B, MVD was calculated according to the fluorescence signaling strength in tumor; C, Correlation analysis between signal-to-noise ratio of MRI and MVD. ** $P < 0.01$ vs. Control.

neighboring water molecules, generate bright contrast on T_1 images. The contrast agents use both linear and macrocyclic ligands, such as DTPA or DOTA [26]. However, they also have the disadvantage that cellular resolution is not provided, making it difficult to find distinct pathologies. Increasing attention has also been paid to PLGA particles as a promising platform for the development of multifunctional devices. Studies have claimed that the acoustic properties can be controlled by controlling the chemical compositions and the molecular weight of the polymers [27,28]. In this study, we tried to construct the contrast agent cRGD-Gd-DTPA-PLGA magnetic nanoparticles used for MRI/ultrasound dual-modality molecular radiography. Clinical contrast agents used for MRI are accompanied with short life span for solid tumors and low aggregation around the tumors due to their low molecular weights [29]. To incorporate the contrast agents into

nanoparticles, we found that the signal intensity was enhanced in vitro and significant target enhancements were achieved in vivo.

Integrin $\alpha\beta_3$ receptors are highly expressed on the surface of tumors and some tumor cells. In recent years, molecular imaging studies of targeted integrins have made great progress, and are gradually applied in clinical practice. Previous studies have revealed that $\alpha\beta_3$ play the role as a unique receptor for the RGD motif, and RGD-containing peptides can specifically bind to integrins with high affinity and are widely used to construct targeted molecular probes, including PET, MRI, ultrasound, and multimodal imaging probes [30]. Based on this, this promising RGD compound targeting $\alpha\beta_3$ can be used for the early tumor imaging and drug delivery of breast cancer [31,32]. For example, a TAB-based cancer-targeting fluorescence probe TAB-3-cRGD has been successfully established and achieved the

specific imaging of cancer cells and the *in vivo* imaging of the U87MG tumor in a mouse model [30]. In this study, we constructed the cRGD-Gd-DTPA-PLGA magnetic nanoparticles used for MRI/ultrasound dual-modality molecular radiography. As a multimodality and stable contrast agent for both MRI and ultrasound imaging, we have demonstrated that cRGD-Gd-DTPA-PLGA magnetic nanoparticles enhanced both the ultrasound imaging and the signal intensity of MRI and relaxation property *in vitro* and *in vivo*. We also revealed the cRGD-Gd-DTPA-PLGA was used for MRI/ultrasound imaging by targeting $\alpha\beta 3$.

In clinical practice, different imaging modes have their own advantages and disadvantages. The use of multi-mode contrast agents for multi-mode imaging has attracted increasing attention. Ultrasound contrast agent can significantly enhance the backscattered signal, and show clearer contrast on the image, complementing ordinary ultrasound information in diagnosis [33]. MRI and MRI-enhanced angiography with good soft tissue resolution, clearly show the lesion with high contrast resolution. Therefore, the dual-mode contrast agent with the function of imaging under ultrasound and MRI may improve the clinical diagnosis and treatment of breast cancer [34]. In this study, cRGD-Gd-DTPA-PLGA magnetic nanoparticles with high safety were constructed, which was capable of performing dual-mode imaging at the same time under both ultrasound and magnetic resonance imaging equipment, and enhanced both the ultrasound imaging and the signal intensity of MRI and relaxation property.

In conclusion, we revealed that cRGD-Gd-DTPA-PLGA could be used as a multimodality and stable contrast agent for MRI/ultrasound dual-modality molecular radiography by targeting $\alpha\beta 3$. This contrast agent enhanced the ultrasound imaging and the signal intensity of MRI and relaxation property *in vitro* and *in vivo*. The signal-to-noise ratio of MRI was positively correlated with MVD, suggesting that cRGD-Gd-DTPA-PLGA dynamically and quantitatively monitored breast cancer in nude mouse model by reflecting the state of neovascularization. The findings of our study

may shed light on the exploration of contrast agents for multimodal imaging.

Conclusion

In summary, we constructed the targeted contrast agent cRGD-Gd-DTPA-PLGA magnetic nanoparticles for MRI/ultrasound dual-modality molecular radiography for the first time. We also demonstrated that cRGD-Gd-DTPA-PLGA magnetic nanoparticles were safe contrast agents for MRI/ultrasound imaging. The cRGD-Gd-DTPA-PLGA nanoparticles bound to the breast cancer cells, and showed qualified results in MRI/ultrasound dual-modality molecular radiography. The cRGD-Gd-DTPA-PLGA was used for MRI/ultrasound imaging by targeting $\alpha\beta 3$. The findings of this study may provide options in the exploration of contrast agents for multimodal imaging.

Acknowledgments

We acknowledge the support from National Natural Science Foundation of China (Grant No. 82,060,311 and 81,971,591), Guangxi Science and Technology Department research program, Guangxi Natural Science Foundation Program (No. 2019GXNSFAA185031), Guangxi Clinical Research Center for Medical Imaging Construction (No. Guike AD20238096) and Guangxi Health Committee Department Self-financing Scientific Research Subject (No. Z20210941).

Disclosure statement

No potential conflict of interest was reported by the author(s).

Funding

National Natural Science Foundation of China (Grant No. 82060311 and 81971591), Guangxi Natural Science Foundation Program (No. Natural Science Foundation of Guangxi Province 2019GXNSFAA185031), Guangxi Clinical Research Center for Medical Imaging Construction (No. Guike AD20238096) and Guangxi Health Committee Department Self-financing Scientific Research Subject (No. Z20210941).

Data availability statement

The datasets generated or analyzed during the study are available from the corresponding author on reasonable request.

References

- [1] Fahad Ullah M. Breast Cancer: current Perspectives on the Disease Status. *Adv Exp Med Biol.* **2019**;1152:51–64.
- [2] Anastasiadi Z, Lianos GD, Ignatiadou E, et al. Breast cancer in young women: an overview. *Updates Surg.* **2017**;69(3):313–317.
- [3] Libson S, Lippman M. A review of clinical aspects of breast cancer. *Int Rev Psychiatry.* **2014**;26(1):4–15.
- [4] MB A, VS R, ME J, et al. Breast cancer biomarkers: risk assessment, diagnosis, prognosis, prediction of treatment efficacy and toxicity, and recurrence. *Curr Pharm Des.* **2014**;20(30):4879–4898.
- [5] Zhang Y, Dong Y, Fu H, et al. Multifunctional tumor-targeted PLGA nanoparticles delivering Pt(IV)/siBIRC5 for US/MRI imaging and overcoming ovarian cancer resistance. *Biomaterials.* **2021**;269:120478.
- [6] Pereira RO, Luz LAD, Chagas DC, et al. Evaluation of the accuracy of mammography, ultrasound and magnetic resonance imaging in suspect breast lesions. *Clinics (Sao Paulo).* **2020**;75:e1805.
- [7] Kuhl CK. Abbreviated Magnetic Resonance Imaging (MRI) for Breast Cancer Screening: rationale, Concept, and Transfer to Clinical Practice. *Annu Rev Med.* **2019**;70(1):501–519.
- [8] Gao Y, Reig B, Heacock L, et al. Magnetic Resonance Imaging in Screening of Breast Cancer. *Radiol Clin North Am.* **2021**;59(1):85–98.
- [9] de Leon A, Perera R, Nittayacharn P, et al. Ultrasound Contrast Agents and Delivery Systems in Cancer Detection and Therapy. *Adv Cancer Res.* **2018**;139:57–84.
- [10] Cai WB, Yang HL, Zhang J, et al. The Optimized Fabrication of Nanobubbles as Ultrasound Contrast Agents for Tumor Imaging. *Sci Rep.* **2015**;5(1):13725.
- [11] Tyler B, Gullotti D, Mangraviti A, et al. Polylactic acid (PLA) controlled delivery carriers for biomedical applications. *Adv Drug Deliv Rev.* **2016**;107:163–175.
- [12] Singhvi MS, Zinjarde SS, Gokhale DV. Polylactic acid: synthesis and biomedical applications. *J Appl Microbiol.* **2019**;127(6):1612–1626.
- [13] Lim EH, Danthi N, Bednarski M, et al. A review: integrin alphavbeta3-targeted molecular imaging and therapy in angiogenesis. *Nanomedicine.* **2005**;1(2):110–114.
- [14] Nieberler M, Reuning U, Reichart F, et al. Exploring the Role of RGD-Recognizing Integrins in Cancer. *Cancers (Basel).* **2017**;9(9):116.
- [15] Hercbegs A. Clinical Implications and Impact of Discovery of the Thyroid Hormone Receptor on Integrin alphavbeta3-A Review. *Front Endocrinol (Lausanne).* **2019**;10:565.
- [16] Mariano RN, Alberti D, Cutrin JC, et al. Design of PLGA based nanoparticles for imaging guided applications. *Mol Pharm.* **2014**;11(11):4100–4106.
- [17] Li Y, Hao L, Liu F, et al. Cell penetrating peptide-modified nanoparticles for tumor targeted imaging and synergistic effect of sonodynamic/HIFU therapy. *Int J Nanomedicine.* **2019**;14:5875–5894.
- [18] Samuel G, Nazim U, Sharma A, et al. Selective Targeting of the Novel CK-10 Nanoparticles to the MDA-MB-231 Breast Cancer Cells. *J Pharm Sci.* **2021**. DOI:10.1016/j.xphs.2021.12.014.
- [19] Chen Y, Tang W, Zhu X, et al. Nuclear receptor binding SET domain protein 1 promotes epithelial-mesenchymal transition in paclitaxel-resistant breast cancer cells via regulating nuclear factor kappa B and F-box and leucine-rich repeat protein 11. *Bioengineered.* **2021**;12(2):11506–11519.
- [20] Ye G, Wang P, Xie Z, et al. IRF2-mediated upregulation of lncRNA HHAS1 facilitates the osteogenic differentiation of bone marrow-derived mesenchymal stem cells by acting as a competing endogenous RNA. *Clin Transl Med.* **2021**;11(6):e429.
- [21] Zhong C, Tao B, Tang F, et al. Remodeling cancer stemness by collagen/fibronectin via the AKT and CDC42 signaling pathway crosstalk in glioma. *Theranostics.* **2021**;11(4):1991–2005.
- [22] Barzaman K, Karami J, Zarei Z, et al. Breast cancer: biology, biomarkers, and treatments. *Int Immunopharmacol.* **2020**;84:106535.
- [23] McPeak PR. Advancements in molecular breast imaging. *Radiol Technol.* **2014**;85(5):523M–538M; quiz 539M–541M.
- [24] Ratzinger G, Agrawal P, Körner W, et al. Surface modification of PLGA nanospheres with Gd-DTPA and Gd-DOTA for high-relaxivity MRI contrast agents. *Biomaterials.* **2010**;31(33):8716–8723.
- [25] Poonaki E, Esfandyar M, Hejazinia H, et al. N-acetylcysteine-PLGA nano-conjugate: effects on cellular toxicity and uptake of gadopentate dimeglumine. *IET Nanobiotechnol.* **2020**;14(6):470–478.
- [26] Cahalane C, Bonezzi J, Shelestak J, et al. Targeted Delivery of Anti-inflammatory and Imaging Agents to Microglial Cells with Polymeric Nanoparticles. *Mol Pharm.* **2020**;17(6):1816–1826.
- [27] Ao M, Wang Z, Ran H, et al. Gd-DTPA-loaded PLGA microbubbles as both ultrasound contrast agent and MRI contrast agent—a feasibility research. *J Biomed Mater Res Part B Appl Biomater.* **2010**;93(2):551–556.
- [28] Li Q, Li C, Tong W. Nile Red Loaded PLGA Nanoparticles Surface Modified with Gd-DTPA for Potential Dual-Modal Imaging. *J Nanosci Nanotechnol.* **2016**;16(6):5569–5576.
- [29] Li X, Feng Q, Jiang X. Microfluidic Synthesis of Gd-Based Nanoparticles for Fast and Ultralong MRI Signals in the Solid Tumor. *Adv Healthc Mater.* **2019**;8(20):e1900672.

- [30] Liu J, Cheng K, Yang C, et al. Application of Triarylboron Substituted with Cyclic Arginine-Glycine-Aspartic Acid Motifs as a Multivalent Two-Photon Fluorescent Probe for Tumor Imaging in Vivo. *Anal Chem.* **2019**;91(9):6340–6344.
- [31] Pathak V, Nolte T, Rama E, et al. Molecular magnetic resonance imaging of Alpha-v-Beta-3 integrin expression in tumors with ultrasound microbubbles. *Biomaterials.* **2021**;275:120896.
- [32] Yadav AS, Radharani NNV, Gorain M, et al. RGD functionalized chitosan nanoparticle mediated targeted delivery of raloxifene selectively suppresses angiogenesis and tumor growth in breast cancer. *Nanoscale.* **2020**;12(19):10664–10684.
- [33] Grabher BJ. Breast Cancer: evaluating Tumor Estrogen Receptor Status with Molecular Imaging to Increase Response to Therapy and Improve Patient Outcomes. *J Nucl Med Technol.* **2020**;48(3):191–201.
- [34] Li X, Xia S, Zhou W, et al. Targeted Fe-doped silica nanoparticles as a novel ultrasound-magnetic resonance dual-mode imaging contrast agent for HER2-positive breast cancer. *Int J Nanomedicine.* **2019**;14:2397–2413.